

Bioinspired Straight Walking Task-Space Planner

Carlo Tiseo^{1,2,*}, Kalyana C Veluvolu³, Wei Tech Ang^{1,2},

1 Rehabilitation Research Institute of Singapore, 50 Nanyang Avenue N3-01a-01, Singapore 639798, Singapore;

2 School of Mechanical & Aerospace Engineering, Nanyang Technological University, 50 Nanyang Avenue N3-01a-01, Singapore 639798, Singapore;

3 School of Electronics Engineering, Kyungpook National University, Daegu 702701, South Korea;

* carlotiseo@gmail.com

Abstract

Although the attention on bipedal locomotion has increased over the last decades, robots are still far behind compared to human locomotor abilities. Their performance limitations can be partially attributed to the hardware, but the primary constrain has been the poor understanding of bipedal dynamics. Based on the recently developed model of potential energy for bipedal structures, this work proposes a task-space planner for human-like straight locomotion. The proposed architecture is based on potential energy model and employs locomotor strategies obtained from human data as a reference for optimal behaviour. The model generates CoM trajectory, foot swing trajectory and the base of support from the knowledge of the desired speed, initial posture, height, weight, number of steps and the angle between the foot and the ground during heel-strike. The data show that the proposed architecture can generate behaviour in line with human walking strategies for both the CoM and the foot swing. Although the planned trajectory is not smooth compared to human trajectories, the proposed model significantly reduces the error in the estimation of the CoM vertical trajectory. Moreover, being the planner able to generate a single stride in less than 140 ms and sequences of 10 strides in less than 600 ms, it allows an online task-space planning for locomotion. Lastly, the proposed architecture is also supported by analogies with current theories on human motor control of locomotion.

1 Introduction

The interest in bipedal equilibrium has been growing exponentially over the last few decades due to the development of bipedal robots and medical technologies targeting locomotor disabilities [8, 17, 27, 36, 44]. The systematic investigation of locomotion strategies started several decades ago. The earlier studies identified the pelvic rotation, pelvic tilt, knee stance flexion, lateral displacement of the pelvis and foot and knee mechanisms as parameters (gait determinants) that characterise the human locomotion and differentiate pathological behaviours [36]. Subsequently, the works focussed on the analysis of the dynamics based on the inverted pendulum model for bipedal locomotion, while the gait determinants were gradually set aside due to their qualitative nature [17, 44]. Models derived from the inverted pendulum model are

currently deployed for both the analysis of human behaviour and bipedal robots controllers [6, 8, 12, 17, 34, 44].

The inverted pendulum does not accurately model the dynamics for step-to-step transition [17]. Therefore, models like the Zero Moment Point (ZMP) and the extrapolated Centre of Mass (XCoM) are required for the extension of the inverted pendulum model to human-like locomotion by identifying the synchronization condition between the legs [6, 14, 17, 32, 44]. However, these models require local optimisation algorithms to plan the walking trajectory in the task space, making the process computationally expensive for highly redundant mechanisms [6, 8, 19, 31]. For example, the algorithm proposed by Carpentier *et al.* [8] requires 4 s for the generation of an optimised solution for a new scenario.

In this paper, we apply a novel analytical model of the potential energy generated by an anthropometric bipedal walker to the formulation of a planner in the task-space [38, 39]. The potential energy model allows to define a posture-dependent reference frame called Saddle Space that is aligned with the principal directions of the potential energy surface, as shown in Figure 1. The y-axis of the Saddle Space (y_{Saddle}) is aligned with the principal direction between the three fixed points of the Saddle, and a stable dynamics characterises the biped in the segment between the two feet. On the other hand, the biped dynamics is always unstable along the x-axis, x_{Saddle} [39–41]. Similar forward planners are available for a non-anthropometric bipedal system like Cornell Ranger [3] that uses the kinematic structure of the Passive Dynamic Walker [27], which has the two legs collinear with the walking direction as described by the inverted pendulum model. The proposed bioinspired task-space planner for straight walking can generate human-like trajectories, and it has been validated using human motion capture data. The choice to initially focus on a straight walking task has been based on the empirical evidence that humans have dedicated alignment strategies for locomotion, which are usually separated by a *quasi*-straight walking path [37]. The planner integrates commonly used parameters such as the XCoM and Base of Support (BoS) to evaluate stability from the locomotion kinematics. Furthermore, the Lyapunov stability analysis is used to demonstrate that the BoS coincides with the system Region of Attraction. Despite the proposed solution has been developed for the assessment of the human locomotor stability from body kinematics, it relies only on the intrinsic mechanical properties of the bipedal structure modelled as two inverted pendula acting on the same mass and can be extended to other bipeds independently from the legs' structures. However, it shall be noted that both stability and optimal strategies depend on the mechanical properties of the biped; thus, they need to be experimentally tuned to each biped.

The paper is organised as follows: in Section 2, the planner architecture and the validation methods are described. The results are presented in Section 3, and discussed in Section 4. Section 5 concludes the paper.

2 Materials and Methods

The planning algorithm is described in the Subsection 2.1 and includes both the generation of the CoM and feet trajectories. It can be noticed from Figure 1 that the proposed method relies only on the Cartesian distances between the Centre of Mass (CoM) and the two Centres of Pressures in the feet (COPs), which are the fulcrums of the two pendula. The stability and the energy analyses derived from the Base of Support (BoS) model introduced in [39] are extended in Section 2.2. Lastly, the methodology used in the evaluation of the planner performances is described in Section 2.3.

2.1 Straight Walking Planning Algorithm

The transversal trajectory of the CoM is obtained by modelling its motion as a harmonic oscillator that moves forward at a constant speed. The planning algorithm divides a 2π cycle of the oscillator into four phases based on the 3 fixed points of the potential energy surface (2 maxima and 1 saddle point [39]). This cycle is exemplified in Figure 2, and every phase is associated with a via point, as follows:

1. *Left Foot Via Point* (L_{Fvp}): It is defined by the desired maximum amplitude of the mediolateral trajectory at the chosen walking velocity during left support, which occurs when both feet are aligned on a segment perpendicular to the walking direction.
2. *Left-to-Right Saddle Via Point* (L_{Svp}): It is defined by the desired saddle position associated with the chosen walking speed. The position of the saddle point is selected under the hypothesis that both pendula have the same maximum length; thus placing it in the middle of the segment connecting the two CoPs [39].
3. *Right Foot Via Point* (R_{Fvp}): It is the equivalent to L_{Fvp} for the right support phase.
4. *Right-to-Left Saddle Via Point* (R_{Svp}): It is defined by the position of the saddle during the transition from right to left support.

The recursive algorithm presented in Figure 3 has been derived from the equation reported in [39] to describe the CoM trajectory in the traverse plane. Once the architecture is defined, it enables the identification of the required inputs and parameters, as shown in Figure 3. Section 2.1.1 describes the equation used for the CoM trajectory, the phase selection and the generation of the swinging trajectory. Section 2.1.2 contains the relationships between the walking velocity with both the step length (d_{SL}) and step width (d_{SW}) which are regressed from the KIT whole-body human motion databases (KITDB) [25], while Section 2.1.3 presents both the models used for the ankle strategies and the CoM vertical trajectory.

Marker set, CoM, CoP and BoS:

The marker set and the method employed to calculate the CoM were derived from the four Iliac Markers used in [25]. Hence, the CoM is placed in the middle of the segment connecting the frontal and the rear centres of the pelvis as defined by Iliac markers. Similarly, the CoPs are calculated as the mid-point along the segments joining the middle of the metatarsus (based on the two metatarsal markers) and the heel marker. It shall be noted that the Centre of Pressure (CoP) is defined as a geometrical point within the foot in our model, and it has been chosen based on the measure of the CoP during standing reported in [12], and as described in [39, 41]. The Base of Support (BoS) is introduced in our formulation in order to represent the range of motion of the CoP in the foot ($\simeq \pm 10$ cm in the anteroposterior direction).

2.1.1 CoM Trajectory Planning:

The desired CoM trajectory generation is based on the following equations [39]:

$$\begin{cases} x_{CoMd}(t) = v_{des}t \\ y_{CoMd}(t) = A_y \cos(\pi\omega_0 t + \phi) \\ z_{CoMd}(t) = \begin{cases} h_{CoML}(t), & \text{if } Left \text{ Support} \\ h_{CoMR}(t), & \text{if } Right \text{ Support} \end{cases} \end{cases} \quad (1)$$

where v_{des} is the desired walking speed, t is the time, and the other parameters are:

1. $\omega_0 = v_{des}/d_{SL}$ is the step cadence, where d_{SL} is the step length.
2. ϕ is the gait phase derived as follows
 - (a) $\phi = 0$: The CoM moves from L_{Fvp} to L_{Svp} .
 - (b) $\phi = \pi/2$: The CoM moves from L_{Svp} to R_{Fvp} .
 - (c) $\phi = \pi$: The CoM moves from R_{Fvp} to R_{Svp} .
 - (d) $\phi = 3\pi/2$: The CoM moves from R_{Svp} to L_{Fvp} .
3. $A_y = d_{SW}/(2\pi\omega_0 d_{SL})$ is the mediolateral amplitude of the CoM movement, where d_{SW} is the step width. The condition is obtained by imposing the trajectory of the CoM is tangent to y_{Saddle} during the step-to-step transition to maximise the stability.
4. $z_{CoMd}(t)$ depends from both the support foot of the gait phase and the length of the pendulum generated by the leg:
 - (a) $h_{CoML}(t) = (h_{LP}(t)^2 - (x_{CoMd}(t) - x_{LCoP}(t))^2 - (y_{CoMd}(t) - y_{LCoP}(t))^2)^{0.5}$
where $x_{LCoP}(t)$ and $y_{LCoP}(t)$ are the coordinates of L_{CoP} .
 - (b) $h_{CoMR}(t) = (h_{RP}(t)^2 - (x_{CoMd}(t) - x_{RCoP}(t))^2 - (y_{CoMd}(t) - y_{RCoP}(t))^2)^{0.5}$
where $x_{RCoP}(t)$ and $y_{RCoP}(t)$ are the coordinates of R_{CoP} .

where both $h_{LP}(t)$ and $h_{RP}(t)$ depend on the ankle strategies explained in Section 2.1.3.

Lastly, the anteroposterior trajectory of the foot is derived based on the hypothesis that the CoM always moves on y_{Saddle} , where the bipedal structure has a stable dynamics (Figure 1) [39]. Therefore, its trajectory is determined based on the condition that its CoP lies on the line connecting the CoM to the CoP that provides support [39].

2.1.2 Regression of Step Length and Step Width from the KITDB:

The analysis of the data from the KITDB, corroborated by the literature, shows a linear relationship between the walking speed and the step length (d_{SL}) [9, 12, 16, 30]. On the other hand, the step width (d_{SW}) shows a more complex highly variable behaviour, which has been connected to both the lateral stabilisation and the energy optimisation of the gait strategies [9, 16].

The data from the KITDB used for this work includes 58 straight walking trajectories, which are collected from 6 different subjects (4 males and 2 females) [25].

Their statistical distribution of age, mass and height are (mean \pm std) 25 ± 2 years, 63.3 ± 10.3 kg, and 1.79 ± 0.10 m.

Our model for the selection of the step width is shown in Figure 4, and it is described by the following equations:

$$d_{SW}(v_{des}) = \begin{cases} 0.22 [m], & v_{des} < 0.6 [m/s] \\ -0.2128v_{des} + 0.3456 [m], & v_{des} \in [0.6, 1.1] [m/s] \\ 0.10 [m], & v_{des} > 1.1 [m/s] \end{cases} \quad (2)$$

where the R^2 of the KITDB data regression is 0.157.

The step length model has been chosen in order to express it as half of the step length. It represents the distance travelled by the CoM in the anteroposterior direction in each of the four phases introduced above. The result of the linear regression used for the generation of the reference behaviour as shown in Figure 5 can be defined as:

$$d_{SL/2}(v_{des}) = \frac{d_{SL}(v_{des})}{2} = 0.1802v_{des} + 0.1351 [m] \quad (3)$$

where the R^2 of the KITDB data regression is 0.98.

2.1.3 Ankle Strategies and CoM Vertical Trajectory Planning:

The ankle strategies are widely regarded to have a fundamental role in both balance and gait efficiency [1, 10, 14, 16, 23, 28, 29, 44]. Therefore, we have decided to investigate the hypothesis that the CoM vertical trajectory error in the inverted pendulum can be mitigated by accounting for the ankle postures in accordance with the following equation:

$$\Delta h_{TO/HS}(t) = \begin{cases} 2d_h \sin(\theta_{TO}(t)/2), & \text{if } \textit{Toe-Off} \\ 2d_h \sin(\theta_{HS}(t)/2), & \text{if } \textit{Heel-Strike} \end{cases} \quad (4)$$

where $d_h = 0.1$ m is the distance of the CoPs from the anterior and the posterior centres of rotation of the foot during Toe-Off and Heel-Strike (HS), respectively [12]. Moreover, θ_{TO} and θ_{HS} are the trajectories of the angles between the feet's soles and the ground during TO and HS respectively, and they are described at the end of this section. Hence, we have modelled the length of the pendulum as follows:

$$\begin{cases} h_{RP}(t) = \begin{cases} l_p + \Delta h_{R_{TO/HS}}(t), & \text{during } TO/HS \\ l_p, & \text{otherwise} \end{cases} \\ h_{LP}(t) = \begin{cases} l_p + \Delta h_{L_{TO/HS}}(t), & \text{during } TO/HS \\ l_p, & \text{otherwise} \end{cases} \end{cases} \quad (5)$$

where $l_p = 0.57h_{body}$ is the length of the pendulum based on anthropometric measures [46], and $\Delta h_{L_{TO/HS}}$ is defined in equation 4.

The parameters required for the generation of the ankle strategies are calculated based on the desired amplitude of the CoM vertical trajectory at the chosen walking speed. This relationship between vertical amplitude and velocity is obtained from the KITDB, as follow:

$$\Delta Z_{CoM}(v_{des}) = 0.02656v_{des} + 0.002575 [m] \quad (6)$$

where R^2 of the KITDB data regression is 0.2015, and it is similar to the behaviour observed by [30]. Then, equation 6 is used to determine the following parameters required to calculate the $\theta_{HS}(t)$ and $\theta_{TO}(t)$.

$$\begin{cases} t_{HS} &= \frac{1}{2\omega_0} - \frac{d_h(1-\cos(\theta_{HS}))}{v_{des}} + t_0 \\ l_{p0} &= ((l_p - \Delta Z_{CoM}(v_{des}))^2 + (x_{CoM_d}(t_{HS}) - x_{CoP0})^2 + \\ &\quad + (y_{CoM_d}(t_{HS}) - y_{CoP0})^2)^{0.5} \\ Max(\theta_{TO}) &= 2 \arcsin(\frac{l_{p0}}{2d_h}) \end{cases} \quad (7)$$

where $Max(\theta_{HS})$ is the Heel Strike angle provided as an input, t_0 is the starting time of the current phase, and x_{CoP0} and y_{CoP0} are the coordinates of the CoP before the starting of the TO, as shown in Figure 6.

The trajectories of the ankle angles have been modelled for both TO and HS strategies with the error function (erf) available in Matlab (Mathworks Inc), as follows:

$$\begin{cases} \theta_{HS}(t) = -Max(\theta_{HS}) \times \text{erf}(\frac{(t-t_{HS})}{0.11}) + Max(\theta_{HS}) \\ \theta_{TO}(t) = Max(\theta_{TO}) \times \text{erf}(\frac{(t-t_{HS})}{0.11}) + Max(\theta_{TO}) \end{cases} \quad (8)$$

where t_{HS} is the instant where the sigmoid curve is centred for the HS, $Max(\theta_{TO})$ is the TO angle when the HS occurs and $Max(\theta_{HS})$ is the desired HS angle provided as input. A sample trajectory for the TO strategy is shown in Figure 8.

2.2 Stability Supervision

The stability analysis for bipeds has always been a challenging problem due to the unavailability of an adequate dynamic model [5, 11, 13, 17, 20, 24, 34, 44]. Therefore, it is difficult to define the general stability criteria, used in the trajectory planning. For example, the ZMP model evaluates the foot placement which is then used to compute the desired CoM trajectory with a stable behaviour via optimisation algorithms [8, 31, 34]. We proposed two kinematic based stability criteria in this work to evaluate if a movement is compatible with stability. Hence, they can be used either for the definition of constraints for motion planning optimisation algorithms or for stability evaluation from the movement kinematics.

2.2.1 XCoM and Step Stability

The step stability during walking is evaluated using the XCoM stability criterion and the maximum reachable distance. In fact, the XCoM allows to identify the minimum step length required for walking at a certain speed [12–14]. That helps to define the criterion for the step stability as shown in Figure 5.

$$d_{SL/2} \in (d_{SL/2_{min}} = \frac{v_d}{2w_n}, d_{SL/2_{Max}}) \quad (9)$$

where w_n is the natural frequency of the inverted pendulum; $d_{SL/2_{min}}$ is half of the minimum step defined by the natural frequency of the pendulum; $d_{SL/2_{Max}}$ is half of the maximum step that can be performed by the biped. This allows us to establish the following metrics for the step stability:

$$\begin{cases} S_{SLP_{end}}(t, v_{CoMp}) = \frac{M_{d_{SL/2}}(t) - d_{SL/2_{min}}(v_{CoMp})}{d_{SL/2}(v_{CoMp}) - d_{SL/2_{min}}(v_{CoMp})} \\ S_{SLJ_{ump}}(t, v_{CoMp}) = \frac{M_{d_{SL/2}}(t) - d_{SL/2_{Max}}(v_{CoMp})}{d_{SL/2}(v_{CoMp}) - d_{SL/2_{Max}}(v_{CoMp})} \end{cases} \quad (10)$$

where v_{CoMp} is the walking velocity, $M_{d_{SL/2}}$ is the half-step length expected as from the biped and $d_{SL/2}$ is the desired behaviour. In summary, equation 9 describes how

to define the stable step length strategies for a generic bipedal structure. On the other hand, equation 10 evaluates selected strategies against an optimal strategy thus providing a quantitative evaluation of the distance from the margins of stability.

2.2.2 Mediolateral Stability

The ML stability evaluation is commonly based on the criterion that the CoM has to be constrained between the two CoPs in the ML direction [14, 21, 26, 45, 47].

$$S_{SW}(t) = 1 - \frac{2|y_{CoM}(t)|}{d_{SW}(v_{CoMp})} \quad (11)$$

2.3 Stability Analysis: Relationship between BoS and Dynamic Stability

The analysis of the system stability is based on the BoS definition that guarantees the necessary condition for stability and its borders are the Margins of Stability (MoS) [39]. In other words, it describes the regions where the system can be stabilised in the absence of external perturbations. To study the stability in the general case, let's consider the system energy described in the following equation:

$$E = U + K + W + E_P \quad (12)$$

where U is the potential energy of the CoM, K is the kinetic energy, W is the active work, and E_P are the external perturbations. Therefore, the condition for achieving stability in a desired posture is:

$$Max(W) \geq U_{MoS} - U_{CoM} - K - E_P \quad (13)$$

where U_{CoM} and U_{MoS} are the potential energies at the current CoM position and expected intersection with MoS, respectively. If the condition in equation 13 cannot be satisfied, then the system cannot reach a static equilibrium in the existing feet posture, and it should be reconfigured. In other words, a biped is stable as long as it is able to actively adsorb the excess energy (equation 13) to stop in the current feet posture, or if it can implement a stable locomotor strategy as described in equations 10 and 11. In conclusion, equation 13 enables to compute the region of attraction that the bipeds can generate around its CoM for a given posture. Further, it serves as a tool for the analysis of movement stability that can be represented as a continuous transition between stable postures.

2.3.1 BoS as Region of Attraction

The region of attraction can be defined as the set of points where the system is Lyapunov stable [22, 24]. If we choose equation 12 as Lyapunov candidate, then the system is stable if and only if the following condition is satisfied:

$$\dot{E} = \dot{U} + \dot{K} + \dot{W} + \dot{E}_P \leq 0 \quad (14)$$

which implies that in the absence of external perturbations. The condition for Lyapunov stability of a trajectory (C) between the points A and B is:

$$W_C \geq U(B) - U(A) + K - K_{des} \quad (15)$$

where W_C is the maximum energy that the system can actively dissipate along C , and K_{des} is the kinetic energy of the desired trajectory.

2.3.2 BoS as Regions of Finite Time Invariance

The region of attraction theory is valid for time-invariant systems, while our model is time variant because the potential energy depends on the body configuration. However, if the system is considered as time-invariant for small time intervals, then this set of points can be defined as a Region of Finite-Time Invariance [22]. This method is commonly used for the control of systems in highly unstructured environments, which can be accurately predicted for short periods of time [22]. Thus, using the BoS as the set of reachable stable points at a given configuration, the gravitational forces can be regarded as time-invariant within the BoS at every instant. Consequently, the BoS considered as a Region of Finite-Time Invariance, and the instantaneous stability can be evaluated using equation 15.

2.3.3 E-BoS for Global Stability and I-BoS for Local Stability:

The region of attraction and the region of finite time invariance introduced above both allows evaluating the stability of the system used in different scenarios.

The region of attraction is more suited for analysing the global stability of a task because it allows the estimation of the margin of stability for the chosen end-posture. Hence, it provides the expected region of attraction (Expected BoS, E-BoS) for a future posture. Instead, the control of the trajectory requires to consider the local stability conditions that take into account both the local dynamics and the unforeseeable perturbation. Therefore the Region of Finite time-invariance (Instantaneous BoS, I-BoS) is required for such evaluation.

An example of locomotion-related scenarios that allows understanding the difference between E-BoS and I-BoS is:

- *Unperturbed walking on a flat surface*: This being a deterministic walking condition, there are no unpredictable external factors; hence, the E-BoS is a sufficient condition for stability.
- *Perturbed gait*: People walking in everyday living environments are subject to a multitude of perturbations that cannot be predicted during planning. If we consider an unexpected push from behind, it introduces an unforeseeable increase in the kinetic energy along the forward direction. Hence, the I-BoS provides local information required from equation 15 to evaluate the system stability and to plan a response strategy in the altered state.

2.4 Simulations

The simulations have been conducted with Matlab 2016 (Mathworks inc., USA) running on a Lenovo Y50 equipped with an Intel i7-4700HQ and 16 GB of memory. The simulation time is calculated with the *run and time* function included in the software. The time step used in the simulations is 80 ms, which is based on the fastest Central Nervous System (CNS) response time to balance perturbations [23, 28].

The simulations have been performed at velocities of 0.7, 1.0, 1.2 and 1.6 [m/s]. The HS angles used are 5, 10 and 15 [deg]. The feet postures have been selected to have the initial gait phase ($Phase_0$) equal to 0. The mean values of the KIT data have been used as value for the body height and the mass parameters. The simulations have been executed for 2 steps or 1 stride, which leads to a change of gait phase from 0 to π , as shown in Figure 10. An additional set of simulations has been performed with the Matlab timing function to evaluate the planning time for 1 and 10 consecutive strides, which includes the stability evaluation with equations 10 and 11. Furthermore, the planner also calculates the gravitational forces and the MoS calculated with the model presented in [39].

3 Results

The results show that our model can reproduce the desired behaviour along the AP direction (Figure 5), while the behaviour along both the ML (Figure 8) is within human variability. The vertical trajectories (Figure 9) are sufficiently accurate for lower speeds, but they extend beyond human variability at the higher velocities. Nevertheless, it is significantly lower than the amplitude obtained with a rigid pendulum. Moreover, Figure 10 shows that the ankle strategies significantly improve the CoM vertical trajectory, they are still not as smooth as the human cycloidal trajectories.

Furthermore, the comparison between a trajectory from the proposed planner (Figure 11) and a human trajectory from KITDB (Figure 12) shows that human planning is consistent with our planner output. The human data also shows the BoS tracks the movements of the CoM allowing the trajectory to occur on a funnel of points of equilibrium, which is a necessary condition for Lyapunov Stability. Lastly, there is a small portion of the trajectory which occurs outside of the BoS. Nonetheless, it does not compromise the global stability of the system, because the swinging leg can reconfigure the system fast enough to drive the state back into the region of attraction before the foot landing occurs. These results suggest that the proposed model captures human planning strategies for both straight walking.

Lastly, the simulation time is 67 ms per step while planning a stride, and it drops to 26.5 ms per step when planning 10 consecutive strides. The analysis of the simulation times also revealed that the majority of simulation time had been spent to calculate the MoS. The time required to plan the trajectories, estimate the gravitational forces and evaluate both ML and AP stability are respectively 8 and 1.1 ms per via point.

4 Discussion

The data obtained validate our hypothesis that it is possible to produce a computationally inexpensive human-like planning for straight walking using the Saddle Space model proposed in [38]. They also confirm our hypothesis that the divergence of the inverted pendulum model from the human behaviour can be justified by the presence of the ankle strategies. Although a simplified model used for the TO and HS movements does not provide an accurate human-like vertical trajectory, it can still generate a potential energy variation coherent with human behaviour Figure 9.

Nonetheless, our results are limited to straight walking. The following general observation in regards to human locomotion can be made:

- Humans tend to maintain the legs movement in synchronization with the CoM trajectory, allowing the CoM to move as close as possible to y_{Saddle} . This enables to have the step-to-step transition along the direction of the ZMP and to control the angular momentums at the same time [32–34, 34, 47]. Furthermore, the alignment of gravitational forces with y_{Saddle} maximises the efficiency of the movement.
- Adequate planning and control of the ankle strategies drastically improves both the stability and efficiency of walking because they have a significant effect on the system energy expenditure. This observation is also supported by other studies, which attribute to the ankle the major energetic contribution during walking [1, 5, 16, 23, 44]
- Our model suggests that humans plan locomotion based on predetermined optimised strategies. This is in agreement with the current motor control

theories based on the observations that human movements are generated from a collection of stereotyped movements called dynamic primitives, which are influenced by external attractors [2, 15, 18, 48].

- The identification of simple kinematics parameters that allow reproducing a human-like walking suggests that locomotion can be regarded as a reaching task which is based on dynamics constraints. This constrains available solutions for the motion planning algorithm and, consequently, reducing the planner computational time.

4.1 Integration in the Hierarchical Control Architecture

The controller of bipedal robots relies on a hierarchical control architecture. The higher modules take care of complex action planning in the task space, and operate at low frequencies. While descending the hierarchical structure, we will encounter faster modules which plan and control less complex actions accordingly to the directives of higher controllers [1, 4]. The proposed method provides a novel approach to higher level planning for human locomotion, which was not possible with previous models. Instead, our model allows to reduce the space of solution for the joint space planner via the introduction of constraints derived from the characterization of the gravitational force field. In other words, the proposed analytical model allows us to identify the desired foot movement for a given CoM trajectory or *vice versa*; this imposes constraints in the joint space and limits the number of available solutions.

The identification of the via points also allows integrating the obstacle avoidance with the step planning via a modified version of elastic bands method proposed for autonomous robot navigation [4, 35]. Such approach should produce a more human-like behaviour in navigation, where humans often diverge from the theoretically optimal trajectory [37]. Figure 9 also implies that the energy cost of a step is greatly affected from an inefficient ankle strategy. This leads us to hypothesise that it is better to implement a suboptimal navigation trajectory towards the final desired posture rather than computing a highly optimised navigation, which may also be invalidated by unforeseeable changes in the environment. For example, it has been recently observed how humans plan their navigations also considering the final position of orientation along the planning. Therefore, they can converge gradually towards the desired trajectory without having a disrupting effect on their locomotion strategies [37].

5 Conclusion

The proposed planner is the first step in the development of a task-space planner for bipedal locomotion by taking advantage of the intrinsic dynamics of the bipedal structure. The next step will be testing its performances once it is integrated with a joint planner, allowing us to benchmark this approach against current architectures. Particularly, we are interested in the integration with the joint planner recently proposed by [42, 43]. Their architecture has been applied to the wrist pointing task, and it uses the interactions between the hand and the environment to locally optimise the trajectory during the task execution. Furthermore, it requires as inputs the desired trajectory in the task space and the expected environmental dynamics. Therefore, their architecture can be integrated with our task space planner with can provide both the desired trajectory of the end effector and the gravitational force field in a single hierarchical planning architecture.

In conclusion, the proposed a bioinspired task-space planner for straight walking that has been proven to produce accurate human-like trajectories. This study also

allowed to identify that low variability behaviours (e.g. Step Length and CoM Transversal Trajectory) are mainly driven by the task-space planning, while high variability is regulated by the lower controller to manage local stability and optimisation (e.g. Step Width and vertical CoM trajectory). Furthermore, methods for the stability supervision and analysis have been defined. Nonetheless, the current results are limited to a simple task, and they do not take account either for joint planning or multiple locomotion strategies. Thus further investigation is required to confirm our preliminary results and to validate the extendibility of this approach to different strategies.

Acknowledgements

This work is extracted from the PhD Thesis of Carlo [38]. The authors would like to thank Mr Michele Xiloyannis for proofreading the paper. This research was supported by the A*STAR-NHG-NTU Rehabilitation Research Grant: "Mobile Robotic Assistive Balance Trainer" (RRG/16018). The research work of Kalyana C. Veluvolu was supported by the National Research Foundation (NRF) of Korea funded by the Ministry of Education, Science and Technology under Grants (NRF-2017R1A2B2006032) and (NRF-2018R1A6A1A03025109).

Conflicts of Interest

The authors declare no conflict of interest.

References

1. J. Ahn and N. Hogan. Walking Is Not Like Reaching: Evidence from Periodic Mechanical Perturbations. *PLoS ONE*, 7(3):e31767, mar 2012.
2. R. Ajemian and N. Hogan. Experimenting with Theoretical Motor Neuroscience. *Journal of Motor Behavior*, 42(6):333–342, oct 2010.
3. P. Bhounsule, J. Cortell, and A. Ruina. Cornell ranger: Implementing energy-optimal trajectory control using low information, reflex-based control. *Dyn Walk. Pensacola*, 2012.
4. O. Brock and O. Khatib. Real-time re-planning in high-dimensional configuration spaces using sets of homotopic paths. In *Proceedings 2000 ICRA. Millennium Conference. IEEE International Conference on Robotics and Automation. Symposia Proceedings (Cat. No.00CH37065)*, volume 1, pages 550–555. IEEE, 2000.
5. T. Buschmann, A. Ewald, A. von Twickel, and A. Büschges. Controlling legs for locomotion—insights from robotics and neurobiology. *Bioinspiration & Biomimetics*, 10(4):041001, jun 2015.
6. S. Caron, Q.-C. Pham, and Y. Nakamura. ZMP Support Areas for Multicontact Mobility Under Frictional Constraints. *IEEE Transactions on Robotics*, pages 1–14, 2016.
7. J. Carpentier, M. Benallegue, and J.-P. Laumond. On the centre of mass motion in human walking. *International Journal of Automation and Computing*, 2017.

-
8. J. Carpentier, S. Tonneau, M. Naveau, O. Stasse, and N. Mansard. A versatile and efficient pattern generator for generalized legged locomotion. In *2016 IEEE International Conference on Robotics and Automation (ICRA)*, pages 3555–3561. IEEE, may 2016.
 9. S. H. Collins and A. D. Kuo. Two Independent Contributions to Step Variability during Over-Ground Human Walking. *PLoS ONE*, 8(8):e73597, aug 2013.
 10. D. Farris, A. Hampton, M. D. Lewek, and G. S. Sawicki. Revisiting the mechanics and energetics of walking in individuals with chronic hemiparesis following stroke: from individual limbs to lower limb joints. *Journal of NeuroEngineering and Rehabilitation*, 12(1):24, 2015.
 11. J. M. Font-Llagunes and J. Kövecses. Dynamics and energetics of a class of bipedal walking systems. *Mechanism and Machine Theory*, 44(11):1999–2019, nov 2009.
 12. A. Hof, M. Gazendam, and W. Sinke. The condition for dynamic stability. *Journal of Biomechanics*, 38(1):1–8, jan 2005.
 13. A. L. Hof. The ‘extrapolated center of mass’ concept suggests a simple control of balance in walking. *Human Movement Science*, 27(1):112–125, feb 2008.
 14. A. L. Hof, R. M. van Bockel, T. Schoppen, and K. Postema. Control of lateral balance in walking. *Gait & Posture*, 25(2):250–258, feb 2007.
 15. N. Hogan and D. Sternad. Dynamic primitives of motor behavior. *Biological Cybernetics*, 106(11-12):727–739, dec 2012.
 16. M. Kim and S. H. Collins. Once-per-step control of ankle-foot prosthesis push-off work reduces effort associated with balance during walking. *Journal of NeuroEngineering and Rehabilitation*, 12(1):43, dec 2015.
 17. A. D. Kuo. The six determinants of gait and the inverted pendulum analogy: A dynamic walking perspective. *Human Movement Science*, 26(4):617–656, aug 2007.
 18. F. Lacquaniti, Y. P. Ivanenko, and M. Zago. Patterned control of human locomotion. *The Journal of Physiology*, 590(10):2189–2199, may 2012.
 19. J.-P. Laumond, N. Mansard, and J. B. Lasserre. Optimization as motion selection principle in robot action. *Communications of the ACM*, 58(5):64–74, apr 2015.
 20. R. Lei, H. David, and K. Laurence. Computational Models to Synthesize Human Walking. *Journal of Bionic Engineering*, 3(3):127–138, sep 2006.
 21. V. Lugade, V. Lin, and L.-s. Chou. Center of mass and base of support interaction during gait. *Gait & Posture*, 33(3):406–411, mar 2011.
 22. A. Majumdar and R. Tedrake. Robust Online Motion Planning with Regions of Finite Time Invariance. In E. Frazzoli, T. Lozano-Perez, N. Roy, and D. Rus, editors, *Algorithmic Foundations of Robotics . . .*, volume 86 of *Springer Tracts in Advanced Robotics*, pages 543–558. Springer Berlin Heidelberg, Berlin, Heidelberg, 2013.
 23. B. E. Maki and W. E. McIlroy. Cognitive demands and cortical control of human balance-recovery reactions. *Journal of Neural Transmission*, 114(10):1279–1296, oct 2007.

-
24. I. R. Manchester, M. M. Tobenkin, M. Levashov, and R. Tedrake. Regions of Attraction for Hybrid Limit Cycles of Walking Robots. *IFAC Proceedings Volumes*, 44(1):5801–5806, oct 2010.
 25. C. Mandery, O. Terlemez, M. Do, N. Vahrenkamp, and T. Asfour. The KIT whole-body human motion database. In *2015 International Conference on Advanced Robotics (ICAR)*, volume 611909, pages 329–336. IEEE, jul 2015.
 26. P. M. McAndrew Young and J. B. Dingwell. Voluntary changes in step width and step length during human walking affect dynamic margins of stability. *Gait & Posture*, 36(2):219–224, jun 2012.
 27. T. McGeer. Passive Dynamic Walking. *The International Journal of Robotics Research*, 9(2):62–82, apr 1990.
 28. W. E. McIlroy, D. C. Bishop, W. R. Staines, A. J. Nelson, B. E. Maki, and J. D. Brooke. Modulation of afferent inflow during the control of balancing tasks using the lower limbs. *Brain research*, 961(1):73–80, jan 2003.
 29. Myunghee Kim and S. H. Collins. Stabilization of a three-dimensional limit cycle walking model through step-to-step ankle control. In *2013 IEEE 13th International Conference on Rehabilitation Robotics (ICORR)*, pages 1–6. IEEE, jun 2013.
 30. M. S. Orendurff, A. D. Segal, G. K. Klute, J. S. Berge, E. S. Rohr, and N. J. Kadel. The effect of walking speed on center of mass displacement. *Journal of rehabilitation research and development*, 41(6A):829–34, 2004.
 31. N. Perrin, O. Stasse, L. Baudouin, F. Lamiroux, and E. Yoshida. Fast Humanoid Robot Collision-Free Footstep Planning Using Swept Volume Approximations. *IEEE Transactions on Robotics*, 28(2):427–439, apr 2012.
 32. M. Popovic, A. Hofmann, and H. Herr. Angular momentum regulation during human walking: biomechanics and control. In *IEEE International Conference on Robotics and Automation, 2004. Proceedings. ICRA '04. 2004*, volume 3, pages 2405–2411 Vol.3. IEEE, 2004.
 33. M. Popovic, A. Hofmann, and H. Herr. Zero spin angular momentum control: definition and applicability. In *4th IEEE/RAS International Conference on Humanoid Robots, 2004.*, volume 1, pages 478–493. IEEE, 2004.
 34. J. Pratt and R. Tedrake. Velocity-Based Stability Margins for Fast Bipedal Walking. In *Fast Motions in Biomechanics and Robotics*, pages 299–324. Springer Berlin Heidelberg, Berlin, Heidelberg, 2006.
 35. S. Quinlan and O. Khatib. Elastic bands: connecting path planning and control. In *[1993] Proceedings IEEE International Conference on Robotics and Automation*, pages 802–807. IEEE Comput. Soc. Press, 1993.
 36. J. B. Saunders, V. T. Inman, and H. D. Eberhart. The major determinants in normal and pathological gait. *The Journal of bone and joint surgery. American volume*, 35-A(3):543–58, jul 1953.
 37. M. Sreenivasa, K. Mombaur, and J.-P. Laumond. Walking Paths to and from a Goal Differ: On the Role of Bearing Angle in the Formation of Human Locomotion Paths. *PLOS ONE*, 10(4):e0121714, apr 2015.

-
38. C. Tiseo. *Modelling of bipedal locomotion for the development of a compliant pelvic interface between human and a balance assistant robot*. PhD thesis, Nanyang Technological University, 2018.
 39. C. Tiseo and W. Ang. The Balance: An energy management task. In *Proceedings of the IEEE RAS and EMBS International Conference on Biomedical Robotics and Biomechatronics*, volume 2016-July, 2016.
 40. C. Tiseo, M. J. Foo, K. C. Veluvolu, and A. W. Tech. A Postural Model for Tracking the Base of Support. In *2018 40th Annual International Conference of the IEEE Engineering in Medicine and Biology Society, EMBC 2018*, 2018.
 41. C. Tiseo, K. C. Veluvolu, and W. T. Ang. Evidence of a “ Clock ” Determining Human Locomotion. In *2018 40th Annual International Conference of the IEEE Engineering in Medicine and Biology Society, EMBC 2018*, 2018.
 42. P. Tommasino and D. Campolo. Human-like pointing strategies via non-linear inverse optimization. In *2016 6th IEEE International Conference on Biomedical Robotics and Biomechatronics (BioRob)*, volume 2016-July, pages 930–935. IEEE, jun 2016.
 43. P. Tommasino and D. Campolo. Task-space separation principle: a force-field approach to motion planning for redundant manipulators. *Bioinspiration & Biomimetics*, 12(2):026003, feb 2017.
 44. D. Torricelli, J. Gonzalez, M. Weckx, R. Jiménez-Fabián, B. Vanderborght, M. Sartori, S. Dosen, D. Farina, D. Lefeber, and J. L. Pons. Human-like compliant locomotion: state of the art of robotic implementations. *Bioinspiration & Biomimetics*, 11(5):051002, aug 2016.
 45. F. B. van Meulen, D. Weenk, E. H. F. van Asseldonk, H. M. Schepers, P. H. Veltink, and J. H. Buurke. Analysis of Balance during Functional Walking in Stroke Survivors. *PLOS ONE*, 11(11):e0166789, nov 2016.
 46. M. Virnavirta and J. Isolehto. Determining the location of the body s center of mass for different groups of physically active people. *Journal of Biomechanics*, 47(8):1909–1913, jun 2014.
 47. M. Vlutters, E. H. F. van Asseldonk, and H. van der Kooij. Center of mass velocity-based predictions in balance recovery following pelvis perturbations during human walking. *The Journal of Experimental Biology*, 219(10):1514–1523, may 2016.
 48. K. E. Zelik, V. La Scaleia, Y. P. Ivanenko, and F. Lacquaniti. Can modular strategies simplify neural control of multidirectional human locomotion? *Journal of Neurophysiology*, 111(8):1686–1702, apr 2014.

Figures

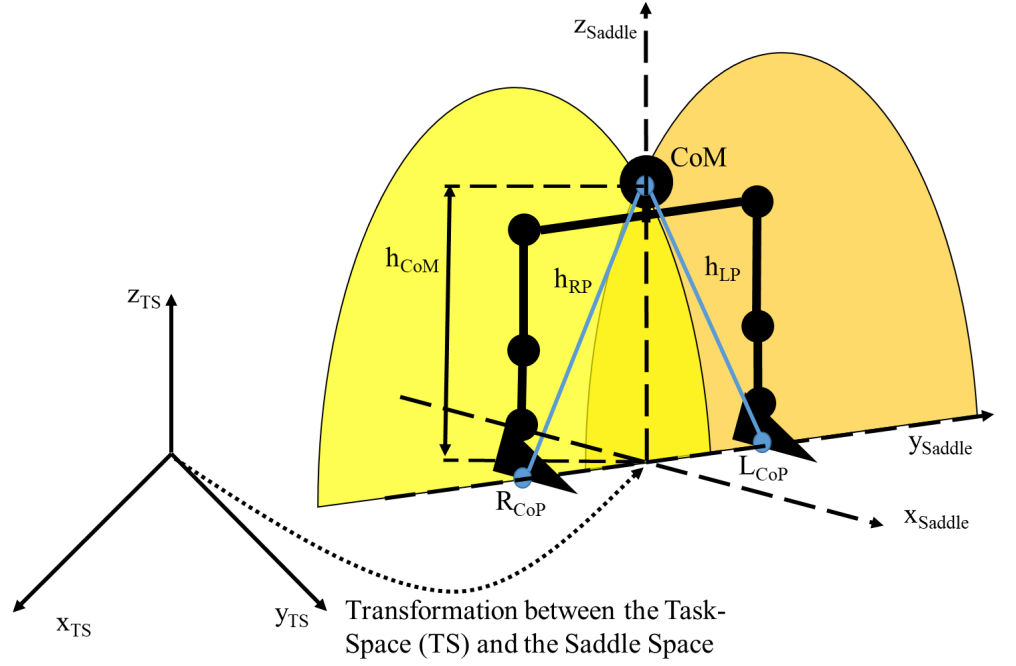


Figure 1. The model relies on the Cartesian formulation of the inverted pendulum which allows the derivation of an analytical model to remove the discontinuity produced by the intersection of the potential energy surface of the two pendula. This is achieved via the definition of a configuration-dependent Saddle Space frame from a generic Task-Space frame. The Saddle Space frame has the y-axis aligned with the principal direction connecting the two fulcra (R_{CoP} and L_{CoP}) and the x-axis lying on the other saddle principal direction. Therefore, the system will have a stable dynamic without any gravitational forces acting on x_{Saddle} direction as long as the CoM trajectory is constrained to the segment connecting the two CoPs [39].

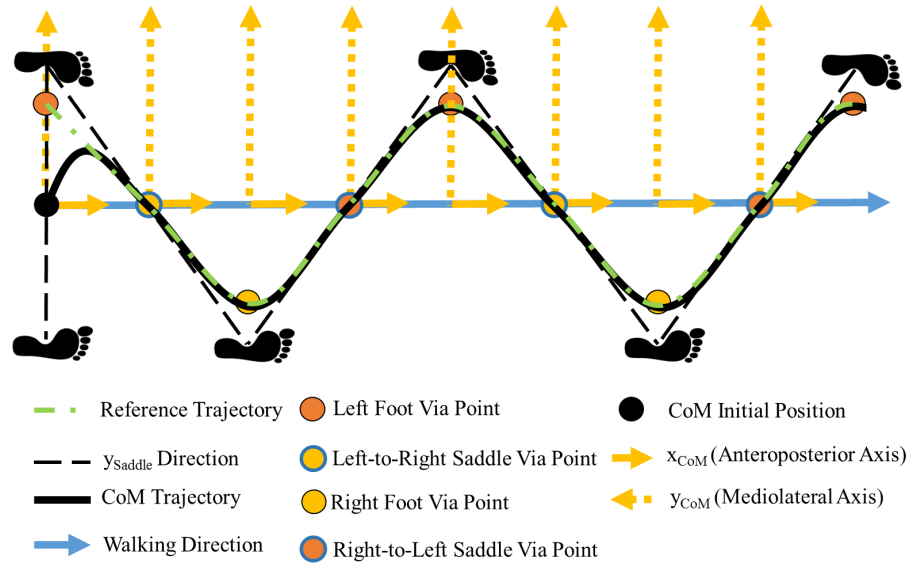


Figure 2. The proposed planner relies on the deployment of the potential energy fixed point to generate the desired trajectories for both the CoM and the swinging foot. This constrains the CoM trajectory to lie on y_{Saddle} that nullifies the gravitational forces perpendicular to the CoM trajectory on the tangent plane [38, 39]. This is used to formulate a recursive algorithm which also optimises the movement energetics.

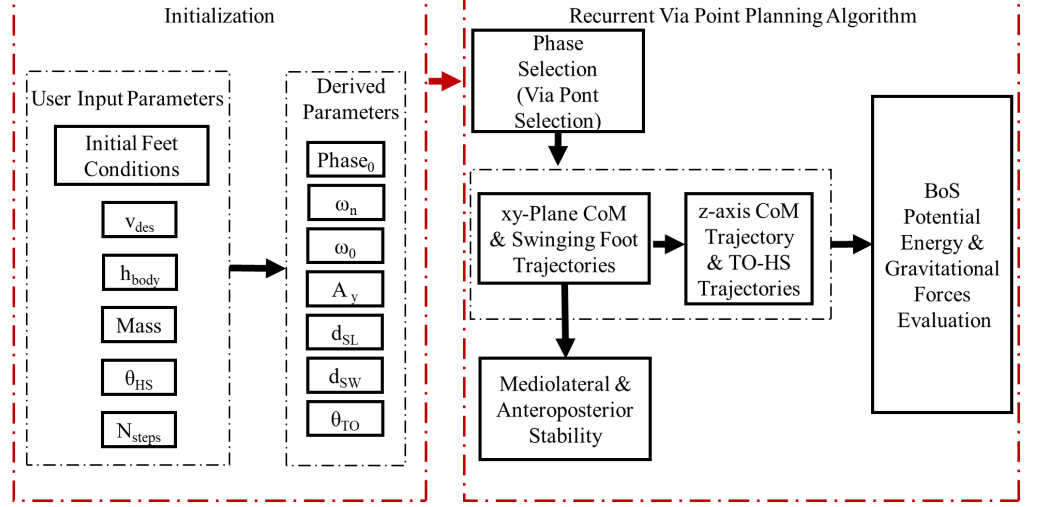


Figure 3. The proposed planner inputs are the initial feet position, the desired velocity, the body height, the mass, the desired HS angle when the foot hits the ground and the number of steps to be simulated. The planning algorithm derives all the other parameters from the inputs, which is explained in Section 2. The $Phase_0$ describes the gait phase (ϕ) used as the initial state for the simulation, and ω_n is the natural frequency of the inverted pendulum. Subsequently, the recurrent module starts from the gait phase selections required for the computation the ankle, the CoM and the Swinging foot trajectories. The derived information is then routed to the two independent modules. The first module uses the foot swing and transversal CoM trajectories to evaluate the Mediolateral (ML) and Anteroposterior stabilities (AL). Instead, the second module computes, the Base of Stability (BoS), the potential energies and the gravitational forces projection along both the axial direction of the pendulum and the tangent plane.

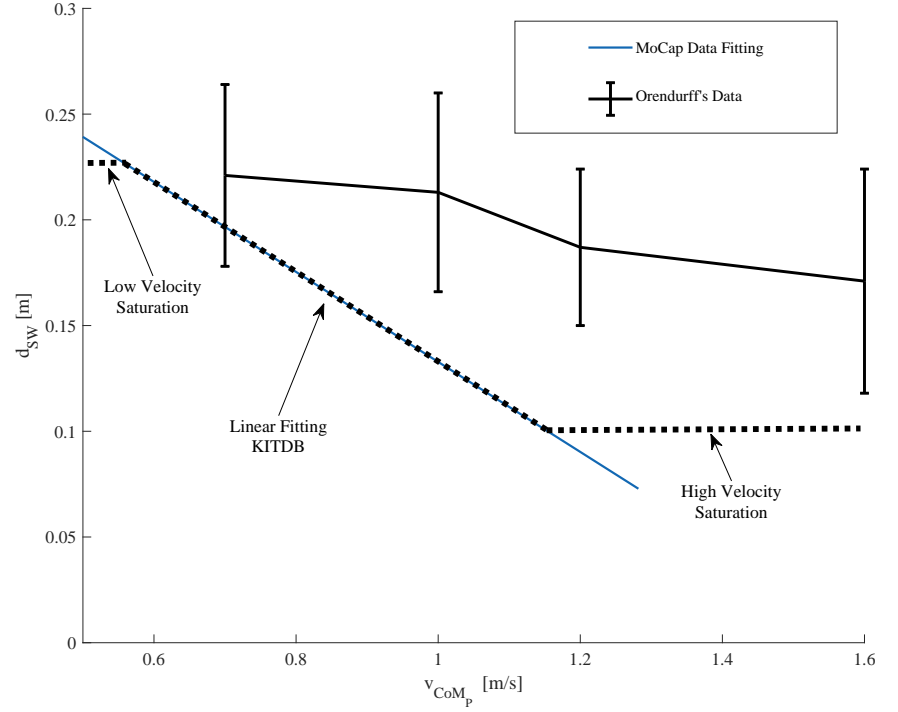


Figure 4. The Step Width (d_{SW}) model is derived from the regression of motion capture data (MoCap Data) from KIT Data Base. Furthermore, the strategy has a general tendency to decrease with the increase of walking speed, but it is also characterised by high variability [9,30]. Consequently, it has been decided to set our planning parameter along the mean and introduce saturations in both high and low walking speeds.

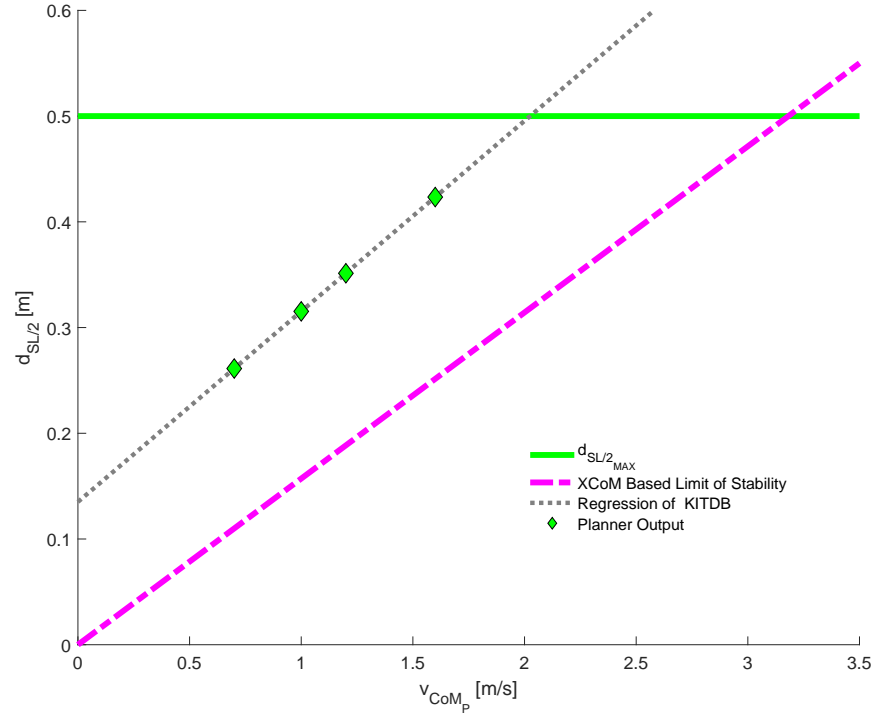


Figure 5. The Step Length (d_{SL}) is a highly regulated behaviour, it has low variability [9], and it has a linear relationship with the velocity. The region of admissible step length extends along the abscissa up to the XCoM limit of stability, and its border along the y-axis is determined by the maximum reachable distance $d_{SL/2_{MAX}}$.

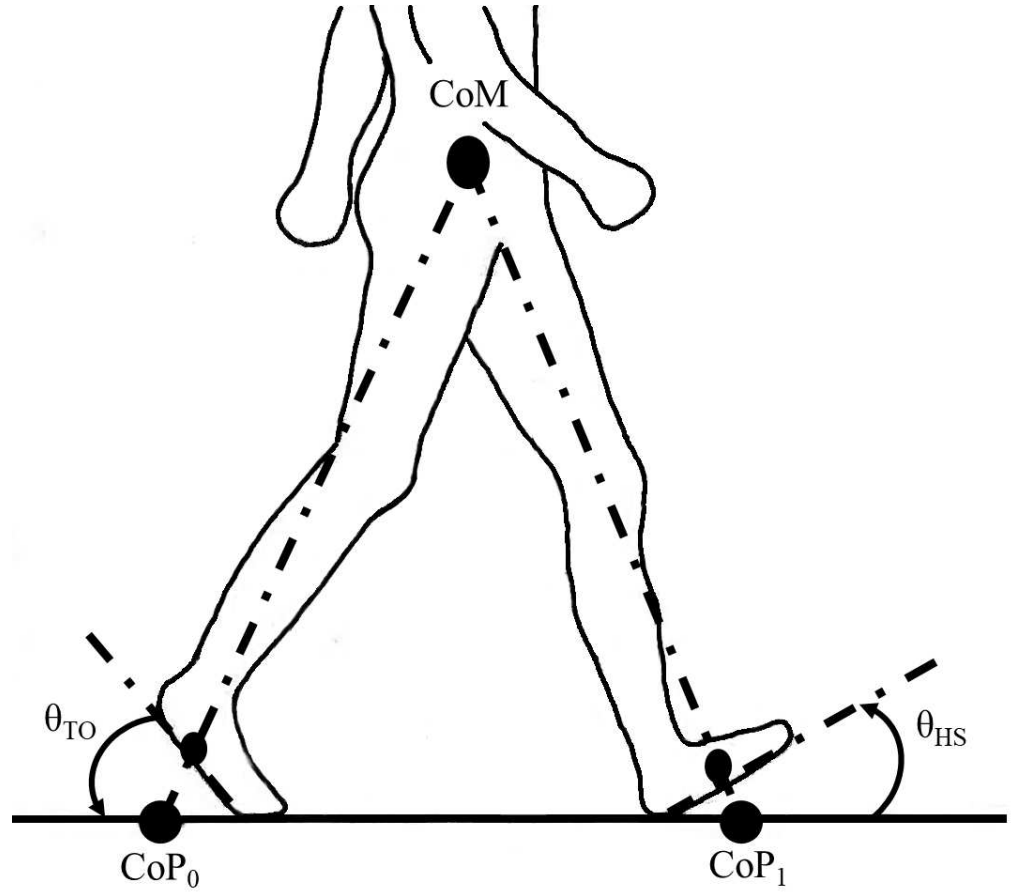


Figure 6. The elongations of the pendulum lengths required for reaching CoP_0 and CoP_1 are derived from the length of the circumference chord, which is centred in the pivoting points with the ground and has a radius $d_h = 0.1$ m. The pivot has been placed in the heel during the HS, and it is located in the articulation between the metatarsus and the phalanges during TO.

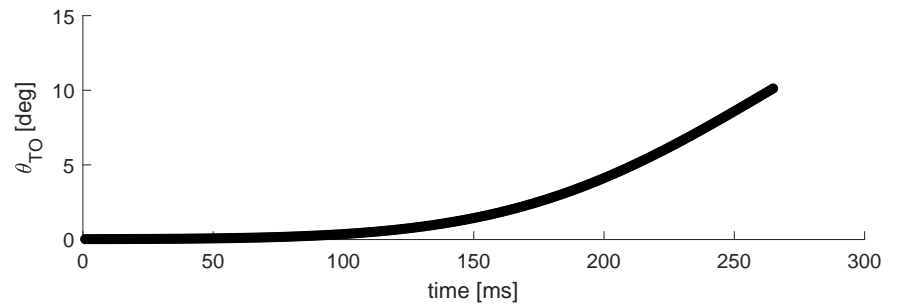


Figure 7. Sample trajectory of the TO angle.

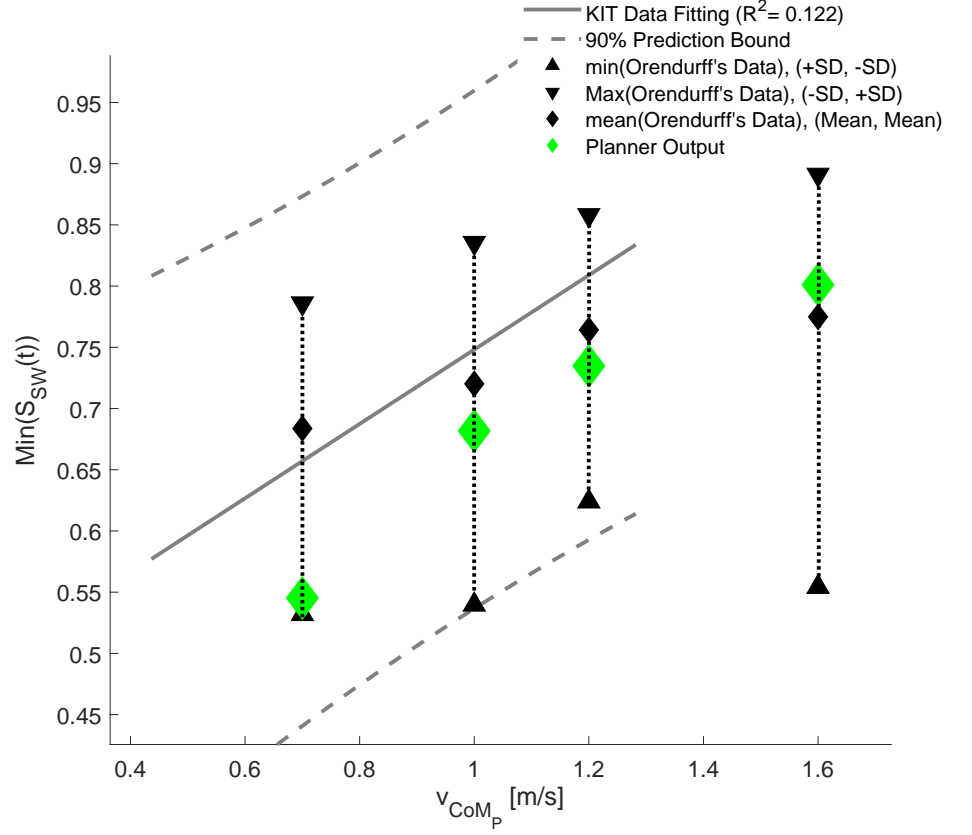


Figure 8. The evaluation of the planner's performance along the mediolateral direction has been conducted by evaluating the minimum of the lateral stability as in equation 11. The results show that our planner can produce a behaviour which is compatible with human data from both the KITDB and Orendurff's data [30].

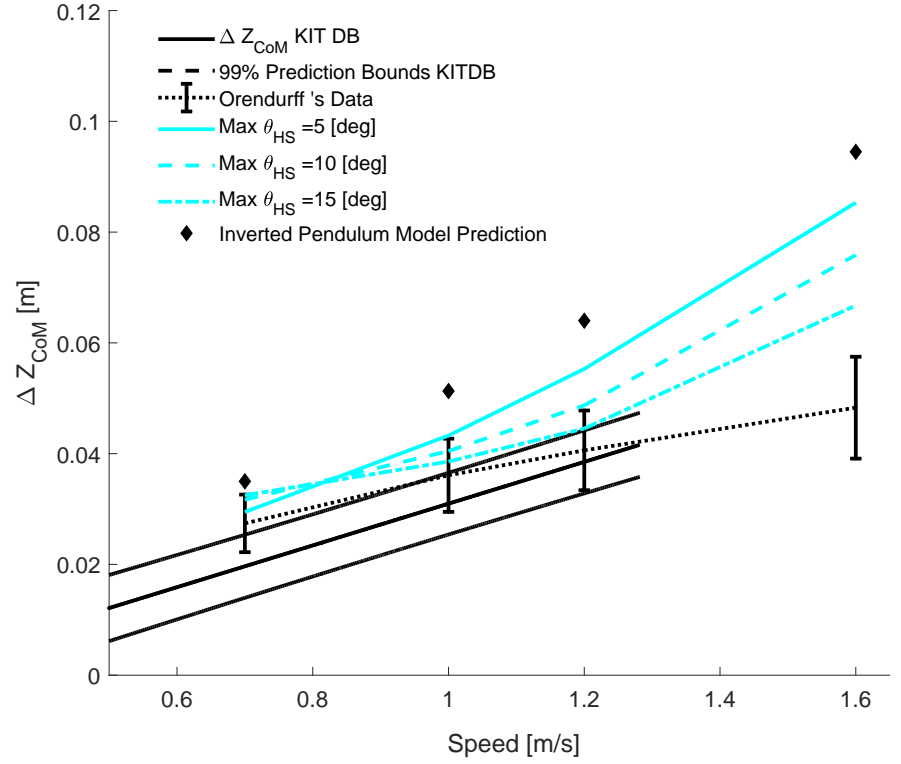


Figure 9. The introduction of the ankle strategies can justify the discrepancy in the vertical CoM trajectories between the human behaviour and the inverted pendulum model. The implementation of this strategy allows humans to increase both the efficiency and the stability of their locomotion. The increased length enables the CoM to reduce the inclination of the leg required to follow the desired trajectory on the transverse plane. Therefore, the ankle strategies allow to minimize the projection of the gravitational force on the tangent plane by redirecting the force along the pendulum axis, where it can be transmitted to the ground via the skeleton. Therefore lowering the muscular effort required for counteracting gravity.

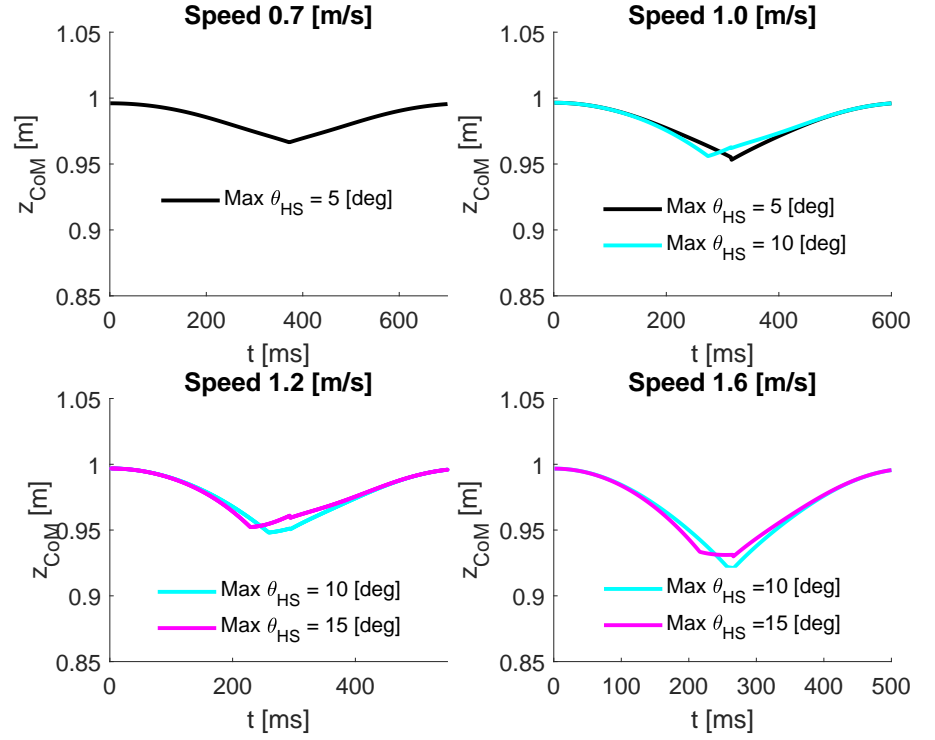


Figure 10. The trajectories of the CoM vertical movements generated from the proposed planner show how the regulation of the ankle strategies during both Toe-Off and Hill-Strike can significantly alter the CoM trajectory. Although the CoM oscillation amplitude is much closer to human behaviour than traditional inverted pendulum models, an improvement in ankle strategies model is still required to obtain a cycloid shape observed in human trajectories [7].

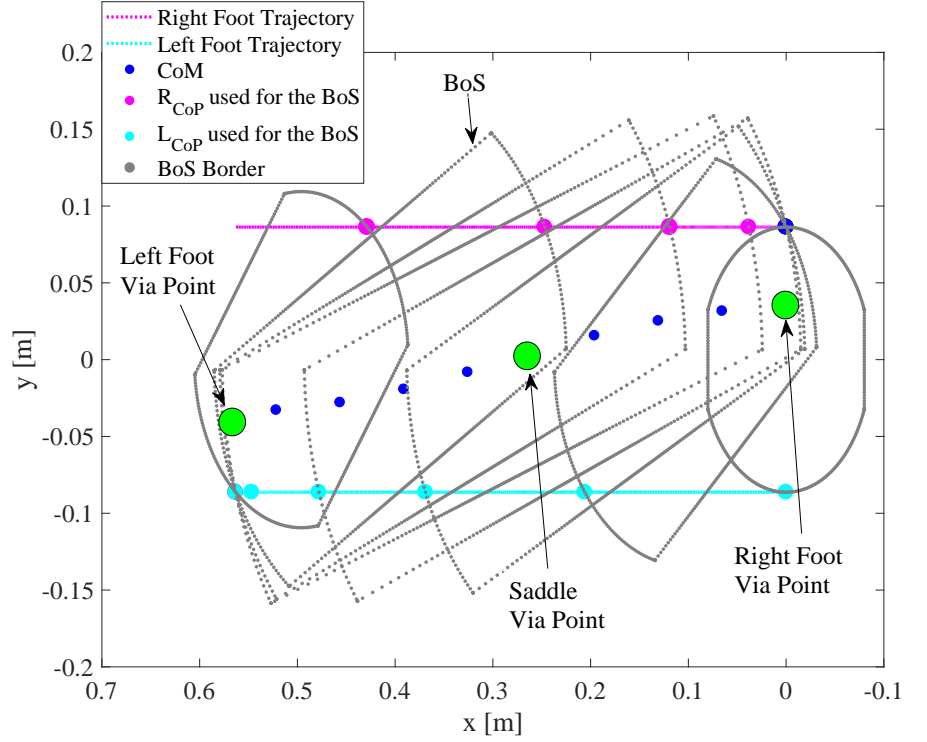


Figure 11. The planner output between the right and left foot via points shows how the movement strategy allows to generate a funnel of stable points between the two legs. The generation of such funnel is necessary for the existence of a stable trajectory leading from one point to the other. The BoS is obtained with the formulation proposed in [39], which is based on experimental data reported by [12].

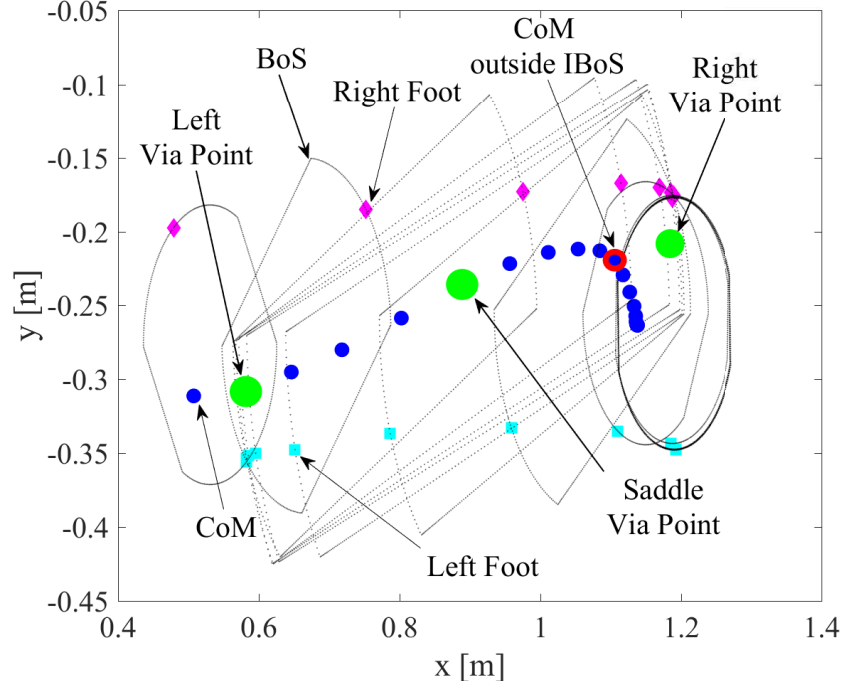


Figure 12. The comparison of the human strategy during gait initiation and the outcome from our planner in Figure 11 shows how the CoM moves towards a trajectory that is consistent with our planner before approaching the saddle via point. This validates our claim that the proposed architecture can produce human-like task-space planning for straight walking trajectories. Furthermore, the analysis of KITDB data also suggests how humans may sometimes desynchronise the swinging leg to deploy the gravitational force to accelerate and decelerate the CoM. For example, this particular trajectory shows how the left foot swing is delayed which allows the CoM to attain a positive abscissa in the saddle space and, consequently, to have the gravitational force to push forward the CoM. Furthermore, this trajectory has also a point that goes beyond the IBoS, which portrays how a local instability does not affect the global stability if the trailing foot it is still able to reach the expected landing position before its support is required. The BoS is obtained with the model proposed in [39], and they are based on the measure of the BoS made by [12].